

hep-ph/0504196

CERN-PH-TH/2005-062

UMN-TH-2352/05

FTPI-MINN-05/10

## On the Interpretation of $B_s \rightarrow \mu^+ \mu^-$ in the CMSSM

John Ellis<sup>1</sup>, Keith A. Olive<sup>2</sup> and Vassilis C. Spanos<sup>2</sup>

<sup>1</sup>*TH Division, CERN, Geneva, Switzerland*

<sup>2</sup>*William I. Fine Theoretical Physics Institute,  
University of Minnesota, Minneapolis, MN 55455, USA*

### Abstract

We discuss the interpretation of present and possible future experimental constraints on  $B_s \rightarrow \mu^+ \mu^-$  decay in the context of the constrained minimal extension of the Standard Model (CMSSM) with universal scalar masses. We emphasize the importance of including theoretical and other experimental uncertainties in calculating the likelihood function, which can affect significantly the inferred 95 % confidence-level limit on the CMSSM parameters. The principal uncertainties are the  $B_s$  meson decay constant,  $m_t$  and  $m_b$ . The latter induce uncertainties in the mass of the neutral Higgs boson that dominates the  $B_s \rightarrow \mu^+ \mu^-$  decay amplitude at large  $\tan \beta$ , reducing the CMSSM region excluded by present and possible future limits from the Fermilab Tevatron collider and the LHC.

CERN-PH-TH/2005-062

July 2005

# 1 Introduction

The prospects for new physics searches at the LHC and other future colliders are already constrained by rare processes that are sensitive to small deviations from the Standard Model. A prime example of such a low-energy constraint is  $b \rightarrow s\gamma$  decay [1,2]. This, the anomalous magnetic moment of the muon,  $g_\mu - 2$  [3], and the Higgs mass,  $m_h$  [4], are among the most important indirect constraints on extensions of the Standard Model, such as the minimal supersymmetric extension of the Standard Model (MSSM).

The decay  $B_s \rightarrow \mu^+\mu^-$  has been emerging as another interesting potential constraint on the parameter space of models for physics beyond the Standard Model, such as the MSSM [5–8]. The Fermilab Tevatron collider already has an interesting upper limit on the branching ratio for  $B_s \rightarrow \mu^+\mu^-$  [9], and is expected soon to increase significantly its sensitivity to  $B_s \rightarrow \mu^+\mu^-$  decay, whilst the LHC sensitivity will reach down to the Standard Model rate [10]. Since its branching ratio is known to increase rapidly for large values of the ratio of Higgs v.e.v.'s,  $\tan\beta$  [11–13], increasing like its sixth power, these present and future sensitivities are particularly important for models with large  $\tan\beta$ .

In view of its potential importance for the MSSM, it is important to treat the  $B_s \rightarrow \mu^+\mu^-$  decay constraint with some care, as has already been done for the  $b \rightarrow s\gamma$ ,  $g_\mu - 2$  and  $m_h$  constraints. In each of these cases, the interpretation depends on uncertainties in theoretical calculations, which should be propagated carefully and combined with the experimental errors if limits are to be calculated at some well-defined confidence level, or if a global fit to MSSM parameters is to be attempted.

Both of these issues are important also in the case of  $B_s \rightarrow \mu^+\mu^-$  decay. As concerns the theoretical uncertainties, it is important to include consistently all the available one-loop MSSM contributions, and avoid any approximate treatments of any individual terms, since cancellations are potentially important, and also to include knowledge of the higher-order QCD corrections to the lowest-order MSSM loop diagrams. As we discuss in this paper, other sources of error and uncertainty are also important. These include, for example, the uncertainties in the  $B_s$  meson parameters, principally the decay constant  $f_{B_s}$ . Since the  $B_s \rightarrow \mu^+\mu^-$  decay rate is dominated by the exchange of the pseudoscalar Higgs boson  $A$ , the value of  $m_A$  is also an important uncertainty.

Bounds on supersymmetry are often explored in a constrained model with universal soft supersymmetry-breaking scalar masses  $m_0$ , gaugino masses  $m_{1/2}$  and trilinear couplings  $A_0$  at some GUT input scale. In this CMSSM, the values of  $m_A$  and magnitude of the Higgs mixing parameter  $\mu$  (but not its sign) are in principle fixed by the electroweak vacuum

conditions. However, these predictions are necessarily approximate. For example, the value of  $m_A$  predicted as a function of the independent parameters  $m_{1/2}, m_0, A_0$  and  $\tan\beta$  has significant uncertainties associated with the lack of precision with which the heavy quark masses  $m_t$  and  $m_b$  are known, as we discuss extensively later in this paper. Moreover, rather different values of  $m_A$  would be predicted in models where the universality assumptions of the CMSSM are relaxed. For example, much smaller values of  $m_A$  are attainable in models with non-universal Higgs masses (NUHM).

When interpreting experimental upper bounds (or measurements) within any specific model such as the CMSSM, care must be taken to incorporate the uncertainties in auxiliary parameters such as  $f_{B_s}, m_t$  and  $m_b$ . These should be propagated and combined with the experimental likelihood function when quoting sensitivities in, e.g., the  $(m_{1/2}, m_0)$  plane at some fixed level of confidence. Moreover, one must also be aware of model dependences within the assumed framework such as the value of  $A_0$  in the CMSSM, as well as the effects of possible deviations from the model framework such as non-universal Higgs masses.

We exemplify these points in a discussion of uncertainties in the interpretation of the present and likely future sensitivities of the Fermilab Tevatron collider and the LHC to  $B_s \rightarrow \mu^+ \mu^-$  decay, assuming  $\mu > 0$  as preferred by  $g_\mu - 2$ . In particular, we show that the uncertainties in  $f_{B_s}, m_t$  and  $m_b$  each shrink significantly the regions that might otherwise appear to be excluded by the present limit, or might appear to be if the decay is not discovered at the likely future sensitivity. We compare the resulting  $B_s \rightarrow \mu^+ \mu^-$  constraints with other existing constraints such as  $b \rightarrow s \gamma$ , discussing how they vary with  $A_0$  and commenting on the situation within the NUHM.

## 2 Calculation of $B_s \rightarrow \mu^+ \mu^-$ Decay

The branching ratio for the decay  $B_s \rightarrow \mu^+ \mu^-$  is given by

$$\begin{aligned} \mathcal{B}(B_s \rightarrow \mu^+ \mu^-) &= \frac{G_F^2 \alpha^2 M_{B_s}^5 f_{B_s}^2 \tau_B}{16\pi^3 4} |V_{tb} V_{ts}^*|^2 \sqrt{1 - \frac{4m_\mu^2}{M_{B_s}^2}} \\ &\times \left\{ \left(1 - \frac{4m_\mu^2}{M_{B_s}^2}\right) |C_S|^2 + \left|C_P - 2C_A \frac{m_\mu}{M_{B_s}^2}\right|^2 \right\}, \end{aligned} \quad (1)$$

where the one-loop corrected Wilson coefficients  $C_{S,P}$  are taken from [13] and  $C_A$  is defined in terms of  $Y(x_t)$ , following [14], as  $C_A = Y(x_t)/\sin^2 \theta_W$  where

$$Y(x_t) = 1.033 \left( \frac{m_t(m_t)}{170 \text{ GeV}} \right)^{1.55}. \quad (2)$$

The function  $Y(x_t)$  incorporates both leading [15] and next-to-leading order [10] QCD corrections, and  $m_t(m_t)$  is the running top-quark mass in the  $\overline{MS}$  scheme. The precise value of  $m_t(m_t)$  depends somewhat on the set of supersymmetric parameters and our choice of the physical top quark mass  $m_t = 178 \pm 4$  GeV [16] that we use in this paper. The Wilson coefficients  $C_{S,P}$  have been multiplied by  $1/(1 + \epsilon_b)^2$ , where  $\epsilon_b$  incorporates the full supersymmetric one-loop correction to the bottom-quark Yukawa coupling [17–19]. It is known that, since  $\epsilon_b$  is proportional to  $\tan \beta$ , this correction may be significant in the large- $\tan \beta$  regime we study here [5,6]. These corrections to  $\epsilon_b$  are flavour independent. In addition, it is important to include the flavour-violating contributions arising from the Higgs and chargino couplings at the one-loop level. These corrections result in effective one-loop corrected values for the Kobayashi-Maskawa (KM) matrix elements [12,20], which we include as described in [21,22]. In particular, these corrections modify the Wilson coefficients involved in Eq. (1), as can be seen in Eqs. (6.35) and (6.36) in [21] or in Eq. (14) in [22]. In addition, the latter study includes the effects of squark mixing, which are included here as well. Below, we discuss the behaviour of the dominant contribution to the Wilson coefficients, mainly to illustrate their dependence on the pseudo-scalar Higgs boson mass.

The Wilson coefficients  $C_{S,P}$  receive four contributions in the context of MSSM, due to Higgs bosons, counter-terms, box and penguin diagrams. The Higgs-boson corrections were calculated in [14], and the rest of the supersymmetric corrections in [11,12]. The full one-loop corrections have been studied and presented comprehensively in [13]. In our numerical analysis, we implement the full one-loop corrections taken from this work as well as the dominant NLO QCD corrections studied in [23], as well as the flavour-changing gluino contribution [22,24]. The Higgs-boson, box and penguin corrections to  $C_{S,P}$  are proportional to  $\tan^2 \beta$ , while the counter-term corrections dominate in the large- $\tan \beta$  limit, as they are proportional to  $\tan^3 \beta$ .

In order to understand the behaviour of the branching ratio in the  $(m_{1/2}, m_0)$  plane in the context of the CMSSM, we focus attention on the counter-terms which are mediated by  $A, H, h$  exchange as seen in Eqs. (5.1) and (5.2) of [13]. As seen in Eq. (5.13) of [13], the  $B_s \rightarrow \mu^+ \mu^-$  decay amplitude  $\propto 1/m_A^2$  in the large- $\tan \beta$  limit, and the decay rate  $\propto 1/m_A^4$ . This underlines the importance of knowing or calculating  $m_A$  as accurately as possible.

The counter-term contribution to  $C_{S,P}$  is given by [13]

$$C_{S,P}^{\text{CT}} = \mp \frac{m_\mu \tan^3 \beta}{\sqrt{2} M_W^2 m_A^2} \sum_{i=1}^2 \sum_{a=1}^6 \sum_{m,n=1}^3 [m_{\tilde{\chi}_i^\pm} D_3(y_{ai}) U_{i2}(\Gamma^{UL})_{am} \Gamma_{imn}^a], \quad (3)$$

where

$$\Gamma_{imn}^a = \frac{1}{2\sqrt{2}\sin^2\theta_W} [\sqrt{2}M_W V_{i1}(\Gamma^{UL\dagger})_{na} - (M_U)_{nn} V_{i2}(\Gamma^{UR\dagger})_{na}] \lambda_{mn}, \quad (4)$$

and  $M_U \equiv \text{diag}(m_u, m_c, m_t)$ .  $U$  and  $V$  are the chargino diagonalization matrices,  $\Gamma^{UL}$  and  $\Gamma^{UR}$  are  $6 \times 3$  squark diagonalization matrices, and  $D_3(x) \equiv x \ln x / (1-x)$ . Additionally,  $y_{ai}$  is defined in Eq. (5.10) of [13] as  $y_{ai} \equiv m_{\tilde{u}_a}^2 / m_{\chi_i^+}^2$ , where  $m_{\tilde{u}_a}^2 \equiv \{m_{\tilde{u}_L}^2, m_{\tilde{c}_L}^2, m_{\tilde{t}_1}^2, m_{\tilde{u}_R}^2, m_{\tilde{c}_R}^2, m_{\tilde{t}_2}^2\}$ . Finally,  $\lambda_{mn} \equiv V_{mb} V_{ns}^* / V_{tb} V_{ts}^*$ .

We can split the counter-term contribution into two terms: one that is proportional to  $M_W$  and another that is proportional to  $m_t$ . Starting with the term whose numerator depends on  $M_W$ , it is easy to see that the non-vanishing terms stem from the following combinations of indices:  $\{a, n, m\} = \{111, 222, 333, 633\}$  and  $i = 1, 2$ . However, the first term  $\{111\}$  is suppressed, as it is proportional to  $\lambda_{11} = V_{ub} V_{us} / V_{tb} V_{ts} \simeq -0.022$ , whereas the second is not suppressed, because it is proportional to  $\lambda_{22} = V_{cb} V_{cs} / V_{tb} V_{ts} \simeq -1$ . Nor are the third and fourth terms suppressed, as they are multiplied by  $\lambda_{33} = 1$ . Thus, the part of the counter-term contribution to the Wilson coefficient that is  $\propto M_W$  is

$$C_S^{CT, M_W} = - \sqrt{2} M_W f \left\{ m_{\chi_1^+} V_{11} U_{12} [\lambda_{22} D_3(y_{21}) + \lambda_{33} (\cos^2 \theta_{\tilde{t}} D_3(y_{31}) + \sin^2 \theta_{\tilde{t}} D_3(y_{61}))] \right. \\ \left. + m_{\chi_2^+} V_{21} U_{22} [\lambda_{22} D_3(y_{22}) + \lambda_{33} (\cos^2 \theta_{\tilde{t}} D_3(y_{32}) + \sin^2 \theta_{\tilde{t}} D_3(y_{62}))] \right\}, \quad (5)$$

where

$$f \equiv \frac{m_\mu \tan^3 \beta}{4M_W^2 \sin^2 \theta_W m_A^2}, \quad (6)$$

and we have ignored in (5) terms that are proportional to  $\lambda_{11}$ . The unitarity of the KM matrix implies that  $\lambda_{11} + \lambda_{22} + \lambda_{33} = 0$ , which for small  $\lambda_{11}$  means  $\lambda_{22} = -\lambda_{33}$ , resulting in the suppression of  $C_S^{CT, M_W}$ .

Turning now to the terms that increase with the charge-2/3 quark masses, we see that the terms with  $n = 3$  (the top-quark contributions) dominate the first- and second-generation terms in  $\Gamma_{imn}^a$ . Specifically, the dominant terms have  $\{a, n, m\} = \{333, 633\}$ . In addition, we notice that the  $i = 2$  part is important, since it is proportional to  $V_{22} U_{22}$ , while the  $i = 1$  term is proportional to  $V_{12} U_{12}$ . Hence it is sufficient to take

$$C_S^{CT, m_t} = m_t f \left( \frac{\sin 2\theta_{\tilde{t}}}{2} \right) m_{\chi_2^+} [D(y_{32}) - D(y_{62})], \quad (7)$$

where we set  $V_{22} \simeq U_{22} \simeq 1$ . The expression (7) is the approximation derived in [6]. The GIM cancellation in (5) means that the counterterm contribution to the Wilson coefficients, which is the dominant one, can be approximated relatively well by (7). However, in our analysis we use the full expressions given in [13], as well as the gluino correction and the flavour-violating corrections to Kobayashi-Maskawa matrix elements as described above.

### 3 Dependence of $m_A$ on $m_t$ and on $m_b$

It is clear from the discussion above that the mass of the pseudoscalar Higgs boson,  $m_A$ , is an important ingredient in calculating the branching ratio for the decay  $B_s \rightarrow \mu^+ \mu^-$ , since it enters in the fourth power in the denominators of the Wilson coefficients  $C_S$  and  $C_P$  in (1). Therefore, to further our discussion of the uncertainties in the  $B_s \rightarrow \mu^+ \mu^-$  branching ratio, we now discuss the uncertainties in the calculated value of  $m_A$ .

The electroweak symmetry breaking conditions may be written in the form:

$$m_A^2 = m_{H_1}^2 + m_{H_2}^2 + 2\mu^2 + \Delta_A \quad (8)$$

and

$$\mu^2 = \frac{m_{H_1}^2 - m_{H_2}^2 \tan^2 \beta + \frac{1}{2} m_Z^2 (1 - \tan^2 \beta) + \Delta_\mu^{(1)}}{\tan^2 \beta - 1 + \Delta_\mu^{(2)}}, \quad (9)$$

where  $\Delta_A$  and  $\Delta_\mu^{(1,2)}$  are loop corrections [19, 25–28]. The exact forms of the radiative corrections to  $\mu$  and  $m_A$  are not needed here, but it is important to note that, at large  $\tan \beta$ , the dominant contribution to  $\Delta_\mu^{(1)}$  contains a term which is proportional to  $h_t^2 \tan^2 \beta$ , whereas the dominant contribution to  $m_A^2$  contains terms proportional to  $h_t^2 \tan \beta$  and  $h_b^2 \tan \beta$ . Therefore, the  $m_{H_2}^2$  term along with a piece proportional to  $h_t^2$  in  $\Delta_\mu^{(1)}$  are dominant in (9) in the large- $\tan \beta$  regime, so  $\mu$  depends rather mildly on  $m_b$ .

We illustrate in Fig. 1 the logarithmic sensitivity of  $m_A$ , namely  $\Delta m_A/m_A$ , to  $m_b$  and  $m_t$  along slices through the  $(m_{1/2}, m_0)$  plane for  $\tan \beta = 57$ ,  $A_0 = 0$  and  $\mu > 0$ . We use as representative errors  $\Delta m_t = 1$  GeV and  $\Delta m_b = 0.1$  GeV. Panel (a) shows the effect of varying  $m_0$  for fixed  $m_{1/2} = 300$  GeV, and panel (b) shows the effect of varying  $m_{1/2}$  for fixed  $m_0 = 400$  GeV.

One can understand the behaviour depicted by employing (8), (9) and the renormalization-group equations (RGEs) that govern the evolution of the  $m_{H_i}$  from  $M_{GUT}$  to  $M_Z$ . The one-loop RGE for  $m_{H_1}^2$  depends on  $h_b$ :

$$\frac{\partial m_{H_1}^2}{\partial \ln Q} = \frac{1}{16\pi^2} \left\{ (-6g_2^2 M_2^2 - \frac{6}{3}g_1^2 M_1^2) + 6|h_b|^2(m_{Q_3}^2 + m_{D_3}^2 + m_{H_1}^2 + A_b^2) \right\}, \quad (10)$$

where we ignore, for simplicity, the  $h_\tau$  contribution, while the RGE for  $m_{H_2}^2$  depends on  $h_t$ :

$$\frac{\partial m_{H_2}^2}{\partial \ln Q} = \frac{1}{16\pi^2} \left\{ (-6g_2^2 M_2^2 - \frac{6}{3}g_1^2 M_1^2) + 6|h_t|^2(m_{Q_3}^2 + m_{U_3}^2 + m_{H_2}^2 + A_t^2) \right\}. \quad (11)$$

We see from (10) that, as  $m_b$  increases, the value of  $m_{H_1}^2$  at  $M_Z$  decreases, tending to decrease  $m_A$  (8). More importantly, the term proportional to  $h_b^2$  in  $\Delta_A$  in (8) is proportional

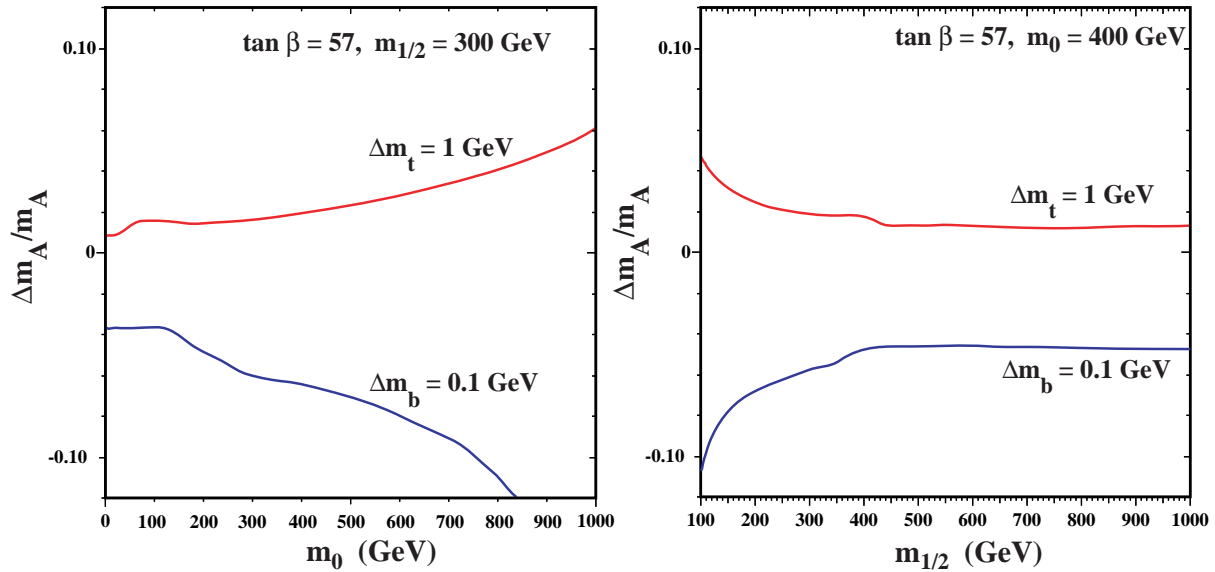


Figure 1: *The sensitivities of  $m_A$  to  $m_t$  and  $m_b$ , assuming  $\Delta m_t = 1$  GeV and  $\Delta m_b = 0.1$  GeV, along slices through the  $(m_{1/2}, m_0)$  CMSSM plane for  $A_0 = 0$  and  $\tan \beta = 57$ . Panel (a) fixes  $m_{1/2} = 300$  GeV and varies  $m_0$ , while panel (b) fixes  $m_0 = 400$  GeV and varies  $m_{1/2}$ .*

to  $m_{b_1}^2 / (m_{b_1}^2 - m_{b_2}^2) \log(m_{b_1}^2 / m_{b_2}^2) - 1$ , which is negative across the  $(m_{1/2}, m_0)$  plane for  $\tan \beta = 57$  and  $A_0 = 0$ , with a magnitude that decreases with  $m_{1/2}$ . Thus, as  $m_b$  increases, we obtain a further decrease in  $m_A$ . This term in fact provides most of the numerical dependence of  $m_A$  on  $m_b$ . Since it is enhanced by  $\tan \beta$ , the  $m_b$  dependence becomes milder for smaller values of  $\tan \beta$ .

In addition, the effect on  $m_A$  is augmented if the role of the bottom Yukawa coupling in the RGE (10) is enhanced, which occurs at large  $m_0$ . This increases the sensitivity of  $m_A$  to  $m_b$ , as seen in Fig. 1(a). In contrast, when  $m_{1/2}$  is increased, the sensitivity to  $\Delta_A$  is diminished and, at the same time, the gaugino part of the RGE is enhanced. Both effects lead to a reduced change in  $m_A$  at large  $m_{1/2}$ , as can be seen in Fig. 1(b).

Turning now to the dependence of  $m_A$  on  $m_t$ , we see that the evolution of  $m_{H_2}^2$  shown in (11) is similar to (10), apart from the substitution of  $h_t$  and analogous mass substitutions. As  $m_t$  increases, the value of  $m_{H_2}^2$  at  $M_Z$  is driven to larger negative values. However, the change in  $m_A$  is dominated by the change in  $\mu$ , which grows with an increase in  $m_t$ . The net effect is an increase in  $m_A$ , as seen in Fig. 1, which increases with  $m_0$  and decreases with  $m_{1/2}$ , as seen in panels (a) and (b), respectively.

Since the  $B_s \rightarrow \mu^+ \mu^-$  decay rate depends on the fourth power of  $m_A$ , the sensitivity of  $m_A$  to both  $m_b$  and  $m_t$  displayed in Fig. 1 can lead to a large uncertainty in  $B_s \rightarrow \mu^+ \mu^-$  for  $\tan \beta = 57$ . We have also evaluated the sensitivities to  $m_t$  and  $m_b$  for  $\tan \beta = 40$ . These

sensitivities do not vary significantly with  $m_{1/2}$  nor with  $m_0$ . They are always smaller than for  $\tan\beta = 57$ , and the difference is rather substantial for large  $m_0$  and small  $m_{1/2}$ .

Numerically, in the following analysis we assume

$$\Delta m_t = 4 \text{ GeV}, \quad \Delta m_b = 0.11 \text{ GeV}, \quad (12)$$

with central values for the physical pole mass  $m_t = 178 \text{ GeV}$  and the running mass  $m_b^{\overline{MS}}(m_b) = 4.25 \text{ GeV}$ . The first of the uncertainties in (12) is taken directly from measurements at the Fermilab Tevatron collider, and may be reduced by a factor of 2 to 4 by future measurements there and at the LHC. The following analysis shows that such reductions would be most welcome also in the analysis of  $B_s \rightarrow \mu^+ \mu^-$  decay. The uncertainty in  $m_b$  is taken from a recent review [29] that combines determinations from  $\bar{b}b$  systems,  $b$ -flavoured hadrons and high-energy processes. Our  $1\text{-}\sigma$  range given in [29] is contained within the preferred range quoted by the Particle Data Group [30], and is very similar to the ranges quoted recently by the UKQCD group [31] in the unquenched approximation and in the review given by Rakow at the Lattice 2004 conference [32].

It is easy to see how important these uncertainties could be. For example, when  $\Delta m_A/m_A = 0.05$  for  $\Delta m_t = 1 \text{ GeV}$ , which occurs when  $\tan\beta = 57$  for  $(m_{1/2}, m_0) = (300, 900)$  or  $(100, 400) \text{ GeV}$ , the change in  $m_A$  for  $|\Delta m_t| = 4 \text{ GeV}$  is  $\pm 0.2 m_A$ , corresponding to a change in the  $A$  contribution to the  $B_s \rightarrow \mu^+ \mu^-$  decay rate by a factor 2.07 or 0.41, depending on the sign of  $\Delta m_t$ .

We note in passing that both the CDF [33] and D0 [34] collaborations have recently published new upper limits on Higgs production at the Fermilab Tevatron collider. In particular, the D0 limit [34] is relevant to the MSSM at very large  $\tan\beta$  and small  $m_A$ . However, such small values of  $m_A$  are already excluded at large  $\tan\beta$  in the CMSSM by other constraints such as  $b \rightarrow s\gamma$  and the lower limit on  $m_h$ , so the present D0 limit does not further restrict the part of the CMSSM parameter space of interest here.

## 4 The Effects of Uncertainties on $B_s \rightarrow \mu^+ \mu^-$ Limits in the CMSSM

In order to assess how important these auxiliary uncertainties may be in the interpretation of  $B_s \rightarrow \mu^+ \mu^-$  experiments, we display in Fig. 2 their individual effects on the present  $B_s \rightarrow \mu^+ \mu^-$  constraint in the  $(m_{1/2}, m_0)$  plane of the CMSSM for  $A_0 = 0$ ,  $\mu > 0$  and  $\tan\beta = 57$ . This is close to the largest value of  $\tan\beta$  for which we find suitable electroweak vacua in generic domains of the  $(m_{1/2}, m_0)$  plane, and so maximizes the potential impact of



the  $B_s \rightarrow \mu^+ \mu^-$  constraint, which increases asymptotically as the sixth power of  $\tan \beta$ . The dark (brick) shaded regions in the bottom-right corners of each panel are excluded because there the lightest supersymmetric particle (LSP) would be the charged  $\tilde{\tau}_1$ . The pale (blue) shaded strips are those favoured by WMAP, if all the cold dark matter is composed of LSPs. The supersymmetric spectrum and relic density calculations have been described elsewhere (see e.g. [35]). The near-vertical dashed (black) lines at small  $m_{1/2}$  are the constraint imposed by the non-observation of charginos at LEP, and the near-vertical dash-dotted (red) lines are those imposed by the non-observation of the lightest MSSM Higgs boson, as calculated using the `FeynHiggs` code [36].

The medium (green) shaded regions are excluded by the rare decay  $b \rightarrow s\gamma$ . The branching ratio for this has been measured by the CLEO, BELLE and BaBar collaborations [1]. The theoretical prediction of  $b \rightarrow s\gamma$  [2, 21, 37] contains uncertainties which stem from the uncertainties in  $m_b$ ,  $\alpha_s$ , the measurement of the semileptonic branching ratio of the  $B$  meson, and the effect of the scale dependence. In particular, the scale dependence of the theoretical prediction arises from the dependence on three scales: the scale where the QCD corrections to the semileptonic decay are calculated and the high and low energy scales relevant to  $b \rightarrow s\gamma$  decay [38]. These sources of uncertainty can be combined to determine a total theoretical uncertainty <sup>1</sup>. The experimental measurement is converted into a Gaussian likelihood and convolved with a theoretical likelihood to determine the total likelihood [40], which is used to calculate the excluded region at 95% CL. It is important to note that the dependence of this excluded region on  $m_A$ ,  $m_b$ , and  $m_t$  is quite weak in comparison, as we have checked numerically.

Finally, the ellipsoidal contours represent the nominal  $B_s \rightarrow \mu^+ \mu^-$  branching ratio, calculated (like all the others) using the current central values  $m_t = 178$  GeV and  $m_b^{\overline{MS}}(m_b) = 4.25$  GeV. The numerical labels for the two outer solid lines are exponents in the branching ratio:  $10^{-7}$ ,  $10^{-8}$ , the thinner-dashed line is for  $2 \times 10^{-8}$ , the thicker-dashed line for  $5 \times 10^{-8}$ .

The most stringent experimental upper bound on the  $B_s \rightarrow \mu^+ \mu^-$  branching ratio is that given by an updated CDF measurement:  $1.5 \times 10^{-7}$  ( $2.0 \times 10^{-7}$ ) at the 90% (95%) CL [9]. The innermost thick solid line of Fig. 2 is the contour for the present nominal 95% CL experimental upper limit of  $2.0 \times 10^{-7}$ .

Panel (a) of Fig. 2 displays as a blue shaded region the effect on the interpretation of the present experimental limit of including the uncertainties in the  $B_s$  meson parameters. The

---

<sup>1</sup>According to a recent analysis [39], these theoretical uncertainties may be significantly larger, resulting to a weaker bound on the masses of supersymmetric particles.

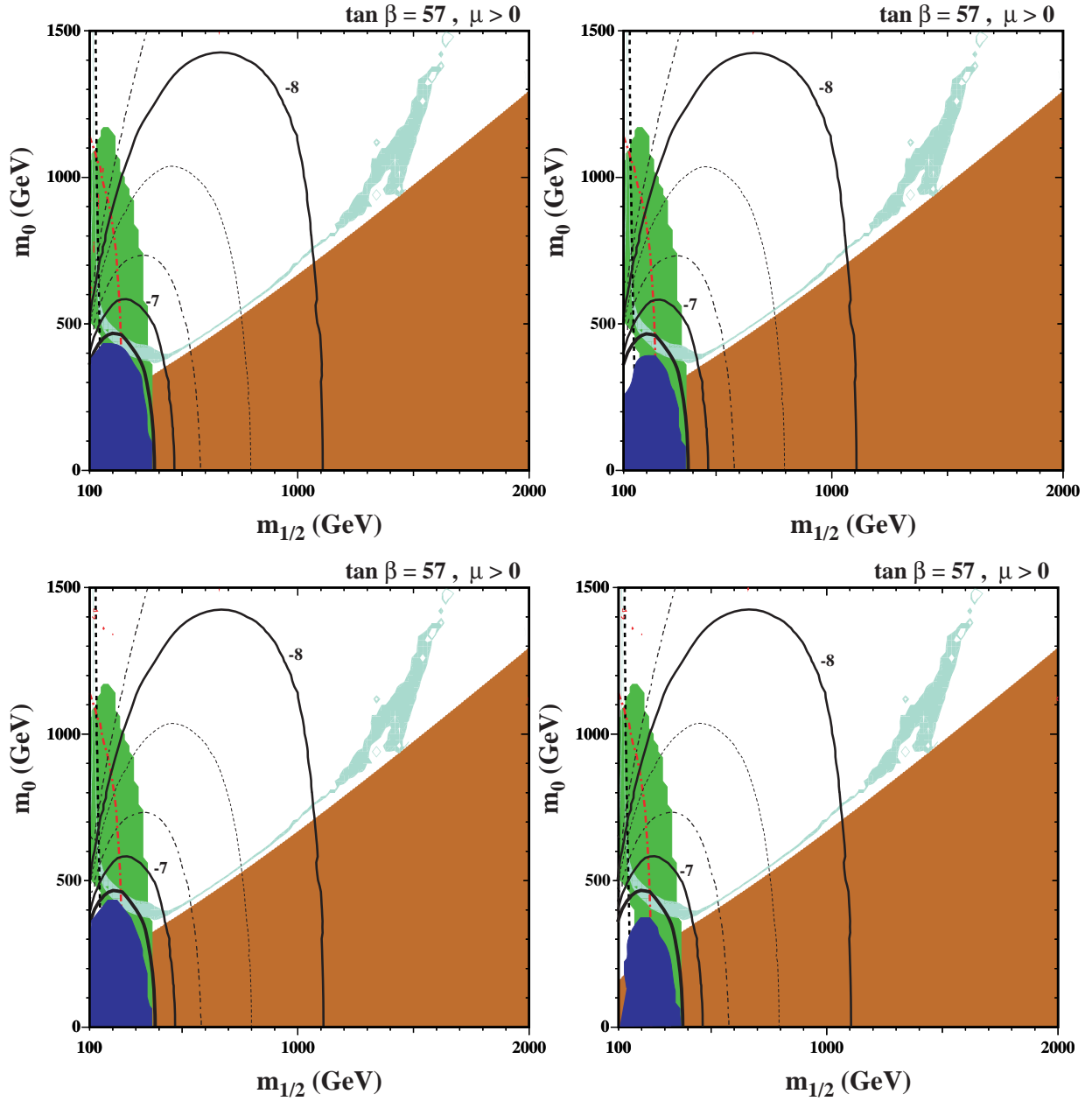


Figure 2: *The effects of auxiliary uncertainties on the region of the  $(m_{1/2}, m_0)$  plane for  $A_0 = 0$ ,  $\mu > 0$  and  $\tan\beta = 57$  currently excluded by the Fermilab Tevatron collider. (a) The effect of  $B_s$  meson uncertainties alone, principally that in  $f_{B_s}$ . (b) These uncertainties combined with the uncertainty  $\Delta m_t = 4$  GeV. (c) The  $B_s$  meson uncertainties combined with the uncertainty  $\Delta m_b = 0.11$  GeV. (d) All uncertainties combined. The various contours and shadings in the  $(m_{1/2}, m_0)$  plane are explained in the text.*

most important uncertainty is that in the decay constant  $f_{B_s}$ , for which we assume [41]

$$f_{B_s} = 230 \pm 30 \text{ MeV}. \quad (13)$$

In addition, we use [30]

$$m_{B_s} = 5369.6 \pm 2.4 \text{ MeV}, \quad \tau_{B_s} = (1.461 \pm 0.057) \times 10^{-12} \text{ s}. \quad (14)$$

In calculating the uncertainty we add quadratically the uncertainties that result from these errors as well as those in the KM elements. We see that incorporating these uncertainties does not change the overall shape of the excluded region, but does shrink it slightly. There may be some possibility to reduce the uncertainty in  $f_{B_s}$  in the foreseeable future, but in this analysis we retain it fixed in the following panels and other figures.

The blue shaded region in panel (b) of Fig. 2 incorporates the present uncertainty in  $m_t$ , assumed to be  $\Delta m_t = 4 \text{ GeV}$ , which is propagated through the CMSSM calculation of  $m_A$  as discussed in the previous Section. We see that this uncertainty is more important for larger  $m_0$ , truncating the upper part of the exclusion domain. This effect can readily be understood from panel (a) of Fig. 1, where we saw that  $\Delta m_t$  has a particularly important effect on  $m_A$  at large  $m_0$ .

The blue shaded region in panel (c) of Fig. 2 shows the parallel effect of the uncertainty in  $m_b$ , assumed to be  $\Delta m_b = 0.11 \text{ GeV}$ , which is also propagated through the CMSSM calculation of  $m_A$  as discussed in the previous Section. This uncertainty is also more important for larger  $m_0$ , providing an independent mechanism for truncating the upper part of the exclusion domain. This can also readily be understood from panel (a) of Fig. 1, where we saw that  $\Delta m_b$  also has a particularly important effect on  $m_A$  at large  $m_0$ .

There is also some tendency in both panels (b) and (c) of Fig. 2 for the exclusion domain to separate from the axis  $m_{1/2} \sim 100 \text{ GeV}$ , particularly at large  $m_0$ . This can be understood from panel (b) of Fig. 1, where we see that the effects of both  $\Delta m_t$  and  $\Delta m_b$  on  $m_A$  are enhanced when  $m_{1/2} \lesssim 200 \text{ GeV}$ . The uncertainties in each of  $m_t$  and  $m_b$  become particularly important when  $m_{1/2}$  is small and  $m_0$  large, as seen separately in panels (b) and (c) of Fig. 2.

The similar tendencies in panels (b) and (c) of Fig. 2 are reinforced when we combine the uncertainties in  $m_t$  and  $m_b$ , as shown by the blue shaded region in panel (d). We find that  $B_s \rightarrow \mu^+ \mu^-$  decay is currently unable to exclude any value of  $m_0$  above about 350 GeV, whereas the exclusion region would have extended up to  $m_0 \sim 450 \text{ GeV}$  if the auxiliary uncertainties had not been taken into account, and  $\sim 400 \text{ GeV}$  if either of the  $m_t$  or  $m_b$  uncertainties had been ignored. On the other hand, the reduction in the excluded range of  $m_{1/2}$  at lower  $m_0$  is less important, typically  $\lesssim 30 \text{ GeV}$ .

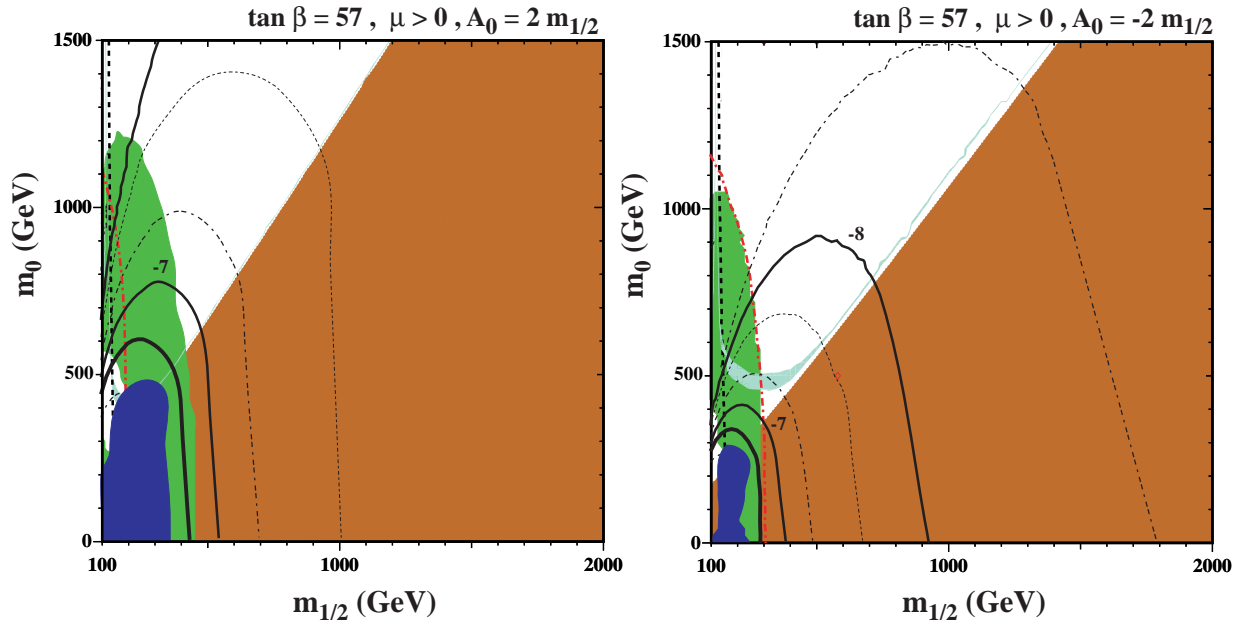


Figure 3: *The disallowed regions in the  $(m_{1/2}, m_0)$  plane for  $\mu > 0$  and  $\tan \beta = 57$ , for (a)  $A_0 = 2m_{1/2}$  and (b)  $A_0 = -2m_{1/2}$ . The various contours and shadings in the  $(m_{1/2}, m_0)$  plane are as explained in the text describing Fig. 2.*

We observe that the region currently excluded by  $B_s \rightarrow \mu^+ \mu^-$  is always included within the region already excluded by  $b \rightarrow s\gamma$  and/or  $m_h$ , even without including the auxiliary uncertainties. The same is even more true for smaller values of  $\tan \beta$ : in the case  $\tan \beta = 40$  (not shown), the region currently excluded by  $B_s \rightarrow \mu^+ \mu^-$  has  $m_{1/2} \lesssim 180$  GeV and  $m_0 \lesssim 170$  GeV, within the strips excluded by  $m_h$  and  $m_{\chi^\pm}$  but allowed by  $b \rightarrow s\gamma$ . We recall that the  $b \rightarrow s\gamma$  limit is very dependent on the assumption of universal scalar masses for the squarks, which does not play a role elsewhere in the analysis of constraints on CMSSM parameters, and is of course untested. Clearly  $B_s \rightarrow \mu^+ \mu^-$  has the potential to complement or even, in the future, supplant the  $b \rightarrow s\gamma$  constraint, though it also relies on squark-mass universality.

The input value of the trilinear soft supersymmetry-breaking parameter  $A_0$  has a significant effect on the allowed CMSSM parameter space, and is also important for  $m_h$  as well as the  $b \rightarrow s\gamma$  and  $B_s \rightarrow \mu^+ \mu^-$  decays. Therefore, we display in Fig. 3 the interplays of these constraints for  $\tan \beta = 57$ ,  $\mu > 0$ , and (a)  $A_0 = 2m_{1/2}$  and (b)  $A_0 = -2m_{1/2}$ . The qualitative conclusions are similar to the  $A_0 = 0$  case discussed previously: the region currently disallowed by  $B_s \rightarrow \mu^+ \mu^-$  decay largely overlaps with the regions previously disfavoured by  $m_h$  and  $b \rightarrow s\gamma$ , and decreases in extent as  $A_0$  is reduced from positive to negative values.

## 5 Treatment of Errors

There are several ways to treat the auxiliary errors in the  $B_s \rightarrow \mu^+ \mu^-$  analysis. In the above, we have implicitly assumed one of the most conservative treatments, in the sense that it excludes the smallest region of the  $(m_{1/2}, m_0)$  plane for given fixed values of the uncertainties. However, other treatments are possible, and here we compare their results. For this comparison, we include all the uncertainties in  $f_{B_s}$ ,  $m_t$  and  $m_b$  discussed in the previous Section.

In our previous treatment, see panel (d) of Fig. 2, we assumed that all the uncertainties have Gaussian error distributions, and defined the allowed region by discarding the upper 2.5% tail of the likelihood distribution obtained by combining the experimental and auxiliary errors. This would be correct if the central value of the experimental measurement, after subtracting any backgrounds, was strictly zero. Alternatively, one might discard the upper 5 % of the combined likelihood distribution. This would give the correct experimental upper limit if the central experimental value were far enough above zero that no significant part of the lower tail of the likelihood distribution extends below zero  $B_s \rightarrow \mu^+ \mu^-$  decay rate, but is otherwise clearly more conservative than the previous treatment. Finally, experimentalists sometimes subtract one theoretical (systematic) error from the measured result and then plot the 95 % confidence-level contour given by the experimental error.

The two alternative prescriptions yield similar upper limits on  $m_0$ , though the shapes of the allowed regions are different. They both reach up to  $m_0 \sim 400$  GeV, as compared the range  $m_0 \lesssim 350$  GeV found in the previous analysis, shown in panel (d) of Fig. 2. We prefer to use the more conservative prescription used in drawing the previous figures, also because it is demonstrably appropriate if the central experimental value is negligible, as is currently the case.

## 6 Possible Future Developments

It is expected that the Fermilab Tevatron collider experiments will continue to improve the present sensitivity to  $B_s \rightarrow \mu^+ \mu^-$  decay. To assess the likely impact of this improved sensitivity, we exhibit in Fig. 4 the potential  $(m_{1/2}, m_0)$  planes for  $A_0 = 0$  and  $\tan \beta = 57, 40$ , obtained using the conservative error prescription and neglecting possible improvements in the determinations of  $f_{B_s}$ ,  $m_t$  and  $m_b$ , in the pessimistic case that no signal is seen.

In panel (a) of Fig. 4 for  $\tan \beta = 57$ , we show that the  $B_s \rightarrow \mu^+ \mu^-$  constraint would, under these pessimistic assumptions, begin to exclude a region in the neighbourhood of

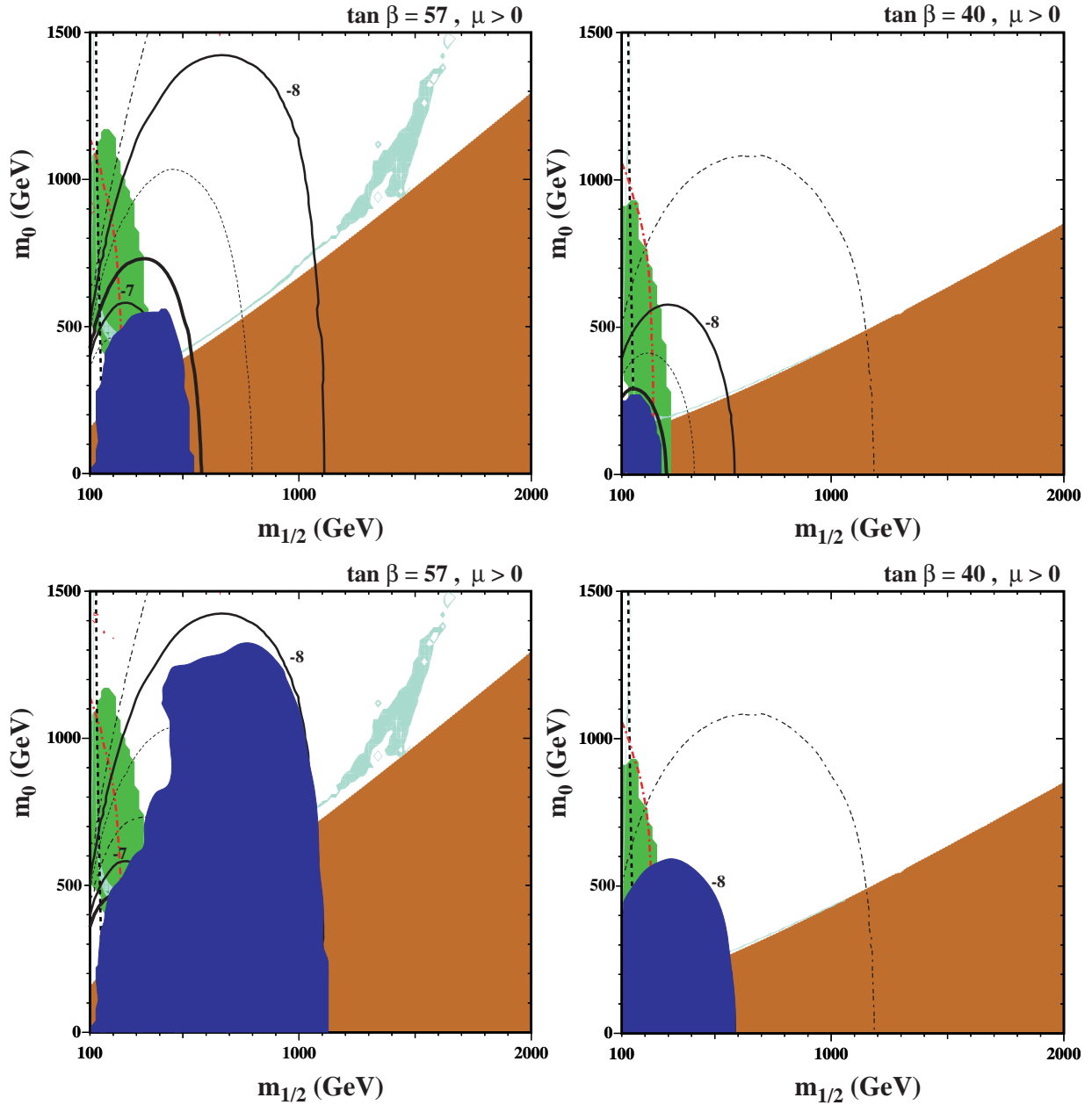


Figure 4: *The potential disallowed regions in the  $(m_{1/2}, m_0)$  plane for  $A_0 = 0, \mu > 0$  and (a)  $\tan \beta = 57$ , (b)  $\tan \beta = 40$ , obtained assuming a Fermilab Tevatron upper limit on  $B_s \rightarrow \mu^+ \mu^-$  that is improved to a 95% CL upper limit of  $5 \times 10^{-8}$ , with no parallel reductions in the uncertainties in  $f_{B_s}$ ,  $m_t$  and  $m_b$ . Panels (c) and (d) show the corresponding disallowed domains assuming a conjectural LHC measurement  $BR(B_s \rightarrow \mu^+ \mu^-) = (3.9 \pm 1.3) \times 10^{-9}$ . The various contours and shadings in the  $(m_{1/2}, m_0)$  plane are as explained in the text describing Fig. 2.*

$(m_{1/2}, m_0) = (400, 400)$  GeV that is favoured by WMAP and allowed by all the other present constraints, assuming a future 95% CL upper limit of  $5 \times 10^{-8}$ . The region at small  $m_{1/2}$  is allowed because of the high sensitivity to  $m_t$  and  $m_b$  seen in panel (b) of Fig. 1. For  $\tan\beta = 40$ , as seen in panel (b) of Fig. 4, the region disallowed by  $B_s \rightarrow \mu^+ \mu^-$  would still lie within the region already disallowed by  $b \rightarrow s\gamma$ . The much reduced sensitivity of  $B_s \rightarrow \mu^+ \mu^-$  decay to  $m_t$  and  $m_b$  at small  $m_{1/2}$  for  $\tan\beta = 40$  implies that there is no allowed ‘gap’ at small  $m_{1/2}$ .

Panels (c) and (d) of Fig. 4 show the corresponding sensitivities at the LHC, assuming a conjectural  $3\text{-}\sigma$  measurement whose central value coincides with the central value predicted by the Standard Model, i.e.,  $BR(B_s \rightarrow \mu^+ \mu^-) = (3.9 \pm 1.3) \times 10^{-9}$ . In panel (c) for  $\tan\beta = 57$  we see that such a measurement would cover a very large fraction (but not all) of the CMSSM parameter space allowed by WMAP. On the other hand, the fraction covered in panel (d) for  $\tan\beta = 40$  is somewhat smaller. Of course, it is quite likely that the present errors in  $f_{B_s}$ ,  $m_t$  and  $m_b$  will be substantially reduced by the time of this ultimate LHC measurement. Reducing the  $f_{B_s}$  error, in particular, would reduce the scope available for a CMSSM contribution, and extend the  $B_s \rightarrow \mu^+ \mu^-$  exclusion region to larger  $m_{1/2}$ .

## 7 Conclusions

We have seen that the interpretation of the present and prospective experimental limits on  $B_s \rightarrow \mu^+ \mu^-$  decay are very sensitive to auxiliary uncertainties, principally those in  $f_{B_s}$ ,  $m_t$  and  $m_b$ . At the present time, these restrict significantly the regions of the CMSSM parameter space that can be excluded by the current upper limit on this decay, and their uncertainties may not be reduced significantly during the remaining operation of the Fermilab Tevatron collider, with the likely exception of  $m_t$ . However, one might hope that the uncertainties in each of  $f_{B_s}$ ,  $m_t$  and  $m_b$  could be reduced by the time the LHC achieves its ultimate sensitivity to  $B_s \rightarrow \mu^+ \mu^-$  decay. As an exercise, we have considered the possibility that their uncertainties might be reduced to  $\Delta f_{B_s} = 10$  MeV,  $\Delta m_t = 1$  GeV and  $\Delta m_b = 0.05$  GeV. In this case, the LHC reach in the  $(m_{1/2}, m_0)$  plane for  $\tan\beta = 57$  would extend to  $m_{1/2} \gtrsim 1400$  GeV along the WMAP strip.

Beyond the framework of the CMSSM, it would be interesting to study the interpretation of the  $B_s \rightarrow \mu^+ \mu^-$  constraint also in the frameworks of more general models, such as those with non-universal Higgs masses (NUHM) <sup>2</sup> [42]. A complete study of the situation within the NUHM would take us beyond the scope of this paper, so we restrict ourselves to a few

---

<sup>2</sup>We expect the situation in the general low-energy effective supersymmetric theory (LEEST) to be similar.

remarks. The models likely to be disfavoured by  $B_s \rightarrow \mu^+ \mu^-$  are those with a low value of  $m_A$  and large  $\tan \beta$ . Such models also tend to predict large neutralino-nucleus scattering cross sections [7]. We have examined a sample of NUHM scenarios that are apparently excluded by the recent CDMS II upper limit on the direct scattering of supersymmetric dark matter, and found that about half of them are excluded by  $B_s \rightarrow \mu^+ \mu^-$ . The next step would be to examine models apparently allowed by CDMS II, to see how many of them are also excluded by  $B_s \rightarrow \mu^+ \mu^-$ . However, for consistency, one should also study the effects on the dark matter scattering cross section of auxiliary uncertainties such as those in  $m_t$  and  $m_b$ , which has not yet been done in the manner described here for  $B_s \rightarrow \mu^+ \mu^-$ . We plan to present elsewhere such a unified treatment of the uncertainties.

## Acknowledgments

The work of K.A.O. and V.C.S. was supported in part by DOE grant DE-FG02-94ER-40823. We would like to thank D. Cronin-Hennessy, C. Sachrajda and M. Voloshin for helpful discussions.

## References

- [1] S. Chen *et al.* [CLEO Collaboration], Phys. Rev. Lett. **87** (2001) 251807 [arXiv:hep-ex/0108032]; P. Koppenburg *et al.* [Belle Collaboration], Phys. Rev. Lett. **93** (2004) 061803 [arXiv:hep-ex/0403004]. B. Aubert *et al.* [BaBar Collaboration], arXiv:hep-ex/0207076.
- [2] M. Ciuchini, G. Degrassi, P. Gambino and G. F. Giudice, Nucl. Phys. B **527** (1998) 21 [arXiv:hep-ph/9710335]; Nucl. Phys. B **534** (1998) 3 [arXiv:hep-ph/9806308]; C. Degrassi, P. Gambino and G. F. Giudice, JHEP **0012** (2000) 009 [arXiv:hep-ph/0009337]; M. Carena, D. Garcia, U. Nierste and C. E. Wagner, Phys. Lett. B **499** (2001) 141 [arXiv:hep-ph/0010003]; P. Gambino and M. Misiak, Nucl. Phys. B **611** (2001) 338; D. A. Demir and K. A. Olive, Phys. Rev. D **65** (2002) 034007 [arXiv:hep-ph/0107329]; F. Borzumati, C. Greub and Y. Yamada, Phys. Rev. D **69** (2004) 055005 [arXiv:hep-ph/0311151]; T. Hurth, Rev. Mod. Phys. **75** (2003) 1159 [arXiv:hep-ph/0212304].
- [3] G. W. Bennett *et al.* [Muon g-2 Collaboration], Phys. Rev. Lett. **92** (2004) 161802 [arXiv:hep-ex/0401008]; M. Davier, S. Eidelman, A. Hocker and Z. Zhang, Eur. Phys. J. C **31** (2003) 503 [arXiv:hep-ph/0308213]; K. Hagiwara, A. D. Martin, D. Nomura and



- T. Teubner, arXiv:hep-ph/0312250; J. F. de Trocóniz and F. J. Ynduráin, arXiv:hep-ph/0402285; K. Melnikov and A. Vainshtein, arXiv:hep-ph/0312226; M. Passera, arXiv:hep-ph/0411168.
- [4] LEP Higgs Working Group for Higgs boson searches, OPAL Collaboration, ALEPH Collaboration, DELPHI Collaboration and L3 Collaboration, Phys. Lett. B **565** (2003) 61 [arXiv:hep-ex/0306033]. *Search for neutral Higgs bosons at LEP*, paper submitted to ICHEP04, Beijing, LHWG-NOTE-2004-01, ALEPH-2004-008, DELPHI-2004-042, L3-NOTE-2820, OPAL-TN-744, [http://lephiggs.web.cern.ch/LEPHIGGS/papers/August2004\\_MSSM/index.html](http://lephiggs.web.cern.ch/LEPHIGGS/papers/August2004_MSSM/index.html).
- [5] A. Dedes, H. K. Dreiner and U. Nierste, Phys. Rev. Lett. **87** (2001) 251804 [arXiv:hep-ph/0108037].
- [6] R. Arnowitt, B. Dutta, T. Kamon and M. Tanaka, Phys. Lett. B **538** (2002) 121 [arXiv:hep-ph/0203069].
- [7] S. Baek, P. Ko and W. Y. Song, Phys. Rev. Lett. **89** (2002) 271801 [arXiv:hep-ph/0205259]; C. S. Huang and X. H. Wu, Nucl. Phys. B **657** (2003) 304 [arXiv:hep-ph/0212220]. S. Baek, Y. G. Kim and P. Ko, JHEP **0502** (2005) 067 [arXiv:hep-ph/0406033].
- [8] H. Baer, C. Balazs, A. Belyaev, J. K. Mizukoshi, X. Tata and Y. Wang, JHEP **0207** (2002) 050 [arXiv:hep-ph/0205325].
- [9] F. Abe *et al.* [CDF Collaboration], Phys. Rev. D **57** (1998) 3811; D. Acosta *et al.* [CDF Collaboration], Phys. Rev. Lett. **93** (2004) 032001 [arXiv:hep-ex/0403032]; V. M. Abazov *et al.* [D0 Collaboration], Phys. Rev. Lett. **94**, 071802 (2005) [arXiv:hep-ex/0410039]; The D0 Collaboration, D0note, 4733-CONF; <http://www-d0.fnal.gov/Run2Physics/WWW/results/prelim/B/B21/B21.pdf>; M. Herndon, The CDF and D0 Collaborations, FERMILAB-CONF-04-391-E. Published Proceedings 32nd International Conference on High-Energy Physics (ICHEP 04), Beijing, China, August 16-22, 2004; The CDF Collaboration, CDF note 7670; <http://www-cdf.fnal.gov/physics/new/bottom/050407.blessed-bsmumu/>.
- [10] G. Buchalla and A.J. Buras, Nucl. Phys. B **400** (1993) 225; M. Misiak and J. Urban, Phys. Lett. B **451** (1999) 161.

- [11] S. R. Choudhury and N. Gaur, Phys. Lett. B **451** (1999) 86 [arXiv:hep-ph/9810307]; C. S. Huang, W. Liao, Q. S. Yan and S. H. Zhu, Phys. Rev. D **63** (2001) 114021 [Erratum-ibid. D **64** (2001) 059902] [arXiv:hep-ph/0006250]; P. H. Chankowski and L. Slawianowska, Phys. Rev. D **63** (2001) 054012 [arXiv:hep-ph/0008046].
- [12] K. S. Babu and C. F. Kolda, Phys. Rev. Lett. **84** (2000) 228 [arXiv:hep-ph/9909476].
- [13] C. Bobeth, T. Ewerth, F. Kruger and J. Urban, Phys. Rev. D **64** (2001) 074014 [arXiv:hep-ph/0104284].
- [14] H. E. Logan and U. Nierste, Nucl. Phys. B **586** (2000) 39 [arXiv:hep-ph/0004139].
- [15] T. Inami, C.S. Lim, Prog. Theor. Phys. **65** (1981) 297; Prog. Theor. Phys. **65** (1981) 1772 (Erratum).
- [16] V. Abazov et al. [D0 Collaboration], *Nature* **429** (2004) 638, hep-ex/0406031; P. Azzi et al. [CDF Collaboration, D0 Collaboration], hep-ex/0404010.
- [17] R. Hempfling, Phys. Rev. D **49** (1994) 6168; L. J. Hall, R. Rattazzi and U. Sarid, Phys. Rev. D **50** (1994) 7048 [arXiv:hep-ph/9306309]; M. Carena, M. Olechowski, S. Pokorski and C. E. M. Wagner, Nucl. Phys. B **426** (1994) 269 [arXiv:hep-ph/9402253]; R. Rattazzi and U. Sarid, Phys. Rev. D **53** (1996) 1553 [arXiv:hep-ph/9505428]; H. Eberl, K. Hidaka, S. Kraml, W. Majerotto and Y. Yamada, Phys. Rev. D **62** (2000) 055006 [arXiv:hep-ph/9912463].
- [18] M. Carena, D. Garcia, U. Nierste and C. E. M. Wagner, Nucl. Phys. B **577** (2000) 88 [arXiv:hep-ph/9912516].
- [19] D. M. Pierce, J. A. Bagger, K. T. Matchev and R. j. Zhang, Nucl. Phys. B **491** (1997) 3 [arXiv:hep-ph/9606211].
- [20] G. Isidori and A. Retico, JHEP **0111**, 001 (2001) [arXiv:hep-ph/0110121]; JHEP **0209** (2002) 063 [arXiv:hep-ph/0208159].
- [21] A. J. Buras, P. H. Chankowski, J. Rosiek and L. Slawianowska, Nucl. Phys. B **659** (2003) 3 [arXiv:hep-ph/0210145].
- [22] J. K. Mizukoshi, X. Tata and Y. Wang, Phys. Rev. D **66** (2002) 115003 [arXiv:hep-ph/0208078].

- [23] C. Bobeth, A. J. Buras, F. Kruger and J. Urban, Nucl. Phys. B **630** (2002) 87 [arXiv:hep-ph/0112305].
- [24] C. Bobeth, T. Ewerth, F. Kruger and J. Urban, Phys. Rev. D **66** (2002) 074021 [arXiv:hep-ph/0204225].
- [25] V. D. Barger, M. S. Berger and P. Ohmann, Phys. Rev. D **49** (1994) 4908 [arXiv:hep-ph/9311269].
- [26] W. de Boer, R. Ehret and D. I. Kazakov, Z. Phys. C **67** (1995) 647 [arXiv:hep-ph/9405342].
- [27] M. Carena, J. R. Ellis, A. Pilaftsis and C. E. Wagner, Nucl. Phys. B **625** (2002) 345 [arXiv:hep-ph/0111245].
- [28] J. R. Ellis, G. Ridolfi and F. Zwirner, Phys. Lett. B **257** (1991) 83; Phys. Lett. B **262** (1991) 477; A. Yamada, Phys. Lett. B **263**, 233 (1991); M. Drees and M. M. Nojiri, Phys. Rev. D **45** (1992) 2482; P. H. Chankowski, S. Pokorski and J. Rosiek, Phys. Lett. B **274** (1992) 191; Phys. Lett. B **286** (1992) 307; A. Dabelstein, Z. Phys. C **67** (1995) 495 [arXiv:hep-ph/9409375]; M. Carena, J. R. Ellis, A. Pilaftsis and C. E. M. Wagner, Nucl. Phys. B **586** (2000) 92 [arXiv:hep-ph/0003180]; A. Katsikatsou, A. B. Lahanas, D. V. Nanopoulos and V. C. Spanos, Phys. Lett. B **501** (2001) 69 [arXiv:hep-ph/0011370].
- [29] A. X. El-Khadra and M. Luke, Ann. Rev. Nucl. Part. Sci. **52** (2002) 201 [arXiv:hep-ph/0208114].
- [30] S. Eidelman *et al.* [Particle Data Group], Phys. Lett. B **592** (2004) 1.
- [31] C. McNeile, C. Michael and G. Thompson [UKQCD Collaboration], Phys. Lett. B **600** (2004) 77 [arXiv:hep-lat/0408025].
- [32] P. E. L. Rakow, Nucl. Phys. Proc. Suppl. **140** (2005) 34 [arXiv:hep-lat/0411036].
- [33] D. Acosta *et al.* [CDF Collaboration], arXiv:hep-ex/0503039.
- [34] V. Abazov *et al.* [D0 Collaboration], arXiv:hep-ex/0504018.
- [35] J. R. Ellis, K. A. Olive, Y. Santoso and V. C. Spanos, Phys. Lett. B **565** (2003) 176 [arXiv:hep-ph/0303043]; J. Ellis, K. A. Olive, Y. Santoso and V. C. Spanos, arXiv:hep-ph/0502001.

- [36] S. Heinemeyer, W. Hollik and G. Weiglein, *Comput. Phys. Commun.* **124** (2000) 76 [arXiv:hep-ph/9812320]; S. Heinemeyer, W. Hollik and G. Weiglein, *Eur. Phys. J. C* **9** (1999) 343 [arXiv:hep-ph/9812472].
- [37] G. D'Ambrosio, G. F. Giudice, G. Isidori and A. Strumia, *Nucl. Phys. B* **645** (2002) 155 [arXiv:hep-ph/0207036].
- [38] A. J. Buras, A. Kwiatkowski and N. Pott, *Phys. Lett. B* **414** (1997) 157 [Erratum-ibid. *B* **434** (1998) 459] [arXiv:hep-ph/9707482].
- [39] M. Neubert, *Eur. Phys. J. C* **40** (2005) 165 [arXiv:hep-ph/0408179].
- [40] J. R. Ellis, T. Falk, G. Gani and K. A. Olive, *Phys. Rev. D* **62** (2000) 075010 [arXiv:hep-ph/0004169].
- [41] C. W. Bernard, *Nucl. Phys. Proc. Suppl.* **94** (2001) 159 [arXiv:hep-lat/0011064]; M. Wingate, C. T. H. Davies, A. Gray, G. P. Lepage and J. Shigemitsu, *Phys. Rev. Lett.* **92** (2004) 162001 [arXiv:hep-ph/0311130].
- [42] J. Ellis, K. Olive and Y. Santoso, *Phys. Lett.* **B539** (2002) 107 [arXiv:hep-ph/0204192].; J. R. Ellis, T. Falk, K. A. Olive and Y. Santoso, *Nucl. Phys.* **B652** (2003) 259 [arXiv:hep-ph/0210205]; D. G. Cerdeno and C. Munoz, *JHEP* **0410** (2004) 015 [arXiv:hep-ph/0405057]; H. Baer, A. Mustafayev, S. Profumo, A. Belyaev and X. Tata, arXiv:hep-ph/0504001.